

Centromere DNA mutations induce a mitotic delay in *Saccharomyces cerevisiae*

(kinetochore/spindle attachment/checkpoint control/cell cycle/chromosome stability)

FORREST SPENCER AND PHILIP HIETER

Department of Molecular Biology and Genetics, The Johns Hopkins University School of Medicine, Baltimore, MD 21205-2185

Communicated by Leland Hartwell, October 3, 1991

ABSTRACT Cytological observations of animal cell mitoses have shown that the onset of anaphase is delayed when chromosome attachment to the spindle is spontaneously retarded or experimentally interrupted. This report demonstrates that a centromere DNA (*CEN*) mutation carried on a single chromosome can induce a cell cycle delay observed as retarded mitosis in the yeast *Saccharomyces cerevisiae*. A 31-base-pair deletion within centromere DNA element II (CDEII Δ 31) that causes chromosome missegregation in only 1% of cell divisions elicited a dramatic mitotic delay phenotype. Other *CEN* DNA mutations, including mutations in centromere DNA elements I and III, similarly delayed mitosis. Single division pedigree analysis of strains containing the CDEII Δ 31 *CEN* mutation indicated that most (and possibly all) cells experienced delay in each cell cycle and that the delay was not due to increased chromosome copy number. Furthermore, a synchronous population of cells containing the CDEII Δ 31 mutation underwent DNA synthesis on schedule with wild-type kinetics, but subsequently exhibited late chromosomal separation and concomitant late cell separation. We speculate that this delay in cell cycle progression before the onset of anaphase provides a mechanism for the stabilization of chromosomes with defective kinetochore structure. Further, we suggest that the delay may be mediated by surveillance at a cell cycle checkpoint that monitors the completion of chromosomal attachment to the spindle.

The mitotic chromosome cycle requires the execution of processes that ensure the accurate maintenance, replication, and segregation of eukaryotic chromosomes. The individual steps are temporally ordered and coordinated with other events in the cell cycle to permit effective cellular reproduction. There is strong evidence in several eukaryotic species for the dependence of later events on the completion of prior ones (reviewed in ref. 1), including those monitored by surveillance systems at cell cycle “checkpoints” ensuring the faithful execution of early events before late processes are initiated. Work characterizing the *RAD9* gene of *Saccharomyces cerevisiae* (1–3), which is required for the cell cycle delay observed in response to DNA damage, has provided the first and most thoroughly described example of a gene required for checkpoint control of cell cycle progression. Several other examples of genetic loci with properties predicted for functions controlling cell cycle progression at surveillance checkpoints have been recently described in budding yeast (4–7). In theory, checkpoint control processes may exert their effects via interaction with the p34 kinase-related signaling pathway governing cell cycle progression (reviewed in ref. 8), in a manner similar to the mechanisms proposed for *FAR1* or *FUS3* in the cell cycle arrest observed in response to mating pheromone (4, 5).

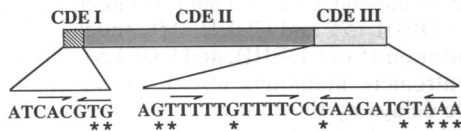
Published cytological observations of animal cell mitoses have implied a connection between the time when all metaphase chromosomes achieve bipolar attachment on the spindle and the onset of anaphase. In these experiments, the spontaneous occurrence of chromosomes retarded in spindle attachment (9), or the experimental interruption of attachment (10, 11), results in a delay before the onset of anaphase. It has been suggested (1) that the anaphase delay exhibited by animal cells in response to a chromosome’s failure in spindle attachment may indicate that the process of kinetochore/microtubule association is similarly governed by a surveillance system.

Although the characteristic trilaminar structures forming the spindle attachment site observed in most eukaryotes (12) have not been visualized in the yeast *S. cerevisiae*, its chromosomes are segregated on a microtubule-based spindle (13) that interacts with the chromosomes via a specific centromeric DNA (*CEN*) sequence (reviewed in ref. 14). Structural and functional analysis of *CEN* DNA from this yeast has identified conserved centromere DNA sequence elements (CDEs; see Fig. 1) within a 125-base-pair segment. Furthermore, the chromosome stability phenotypes of over 50 *CEN* DNA mutations have been characterized, with effects on chromosome transmission fidelity ranging from unaffected to highly defective (14). In the present work, a subset of these defined centromere DNA mutations is used to test the effects of impaired function of the centromeric DNA and its associated proteins on cell cycle progression. We find that centromere DNA mutations induce a delay near the metaphase/anaphase transition and suggest that this delay may be mediated by a surveillance system that monitors the completion of chromosomal attachment to the spindle.

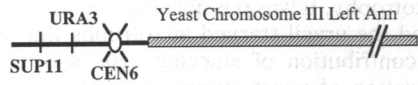
MATERIALS AND METHODS

Yeast Strains and Culture Media. All yeast strains employed were near-isogenic relatives, derived from a common genetic background by DNA-mediated transformation and crosses involving only transformed relatives. The wild-type and mutant *CEN* DNA sequences tested for cell cycle effects were present on either a nonessential disomy for the left arm of chromosome III (15), referred to as a chromosome fragment (CF), or on a yeast artificial chromosome (YAC) as shown in Fig. 1. Experimental and control strains (most of which have been described; refs. 16–19) differed only at the CF *CEN6* sequence. Full genotypes are available upon request. Yeast media were prepared as described (20), and cultures were maintained at 30°C.

Morphological Screen of Fixed Populations. Yeast strains were grown under selection for the CF in minimal medium lacking uracil. Cells in logarithmic growth ($0.5\text{--}2.0 \times 10^6$ per ml) were fixed by addition of 1/10th volume of 37% formal-

A. *CEN6* Structure

B. Chromosome Fragment (150 kb)



YAC12 Derivative (365 kb)

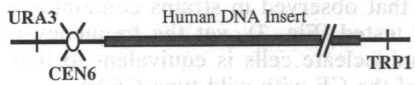


FIG. 1. (A) Yeast *CEN6* (15) showing CDEI, CDEII, and CDEIII drawn to scale (reviewed in ref. 14). The wild-type *CEN6* DNA sequences of CDEI and CDEIII are shown. Stars mark the positions of base substitutions in the mutants shown in Fig. 3. (B) Structures of the test chromosomes. Inclusion of the *SUP11* gene on the CFs allowed the use of a colony color assay for visual monitoring of CF stability and copy number (16). kb, kilobases.

dehydrate (Sigma) to the culture medium. After 2 hr at room temperature, the cells were washed twice in SK (1 M sorbitol/50 mM potassium phosphate, pH 7.5). Samples were treated with zymolyase (100,000 lytic units/g; ICN) at 3 μ g/ml in SK for 10 min at room temperature, washed twice in SK, and stained with 4',6-diamidino-2-phenylindole (DAPI; Sigma) at 300 ng/ml in SK.

The bud size (phase optics) and the number and location of the chromosomal DNA masses (DAPI fluorescence) were determined for each cell. Fixed samples were scored without knowledge of the particular *CEN* DNA mutation present. The relative bud size was determined by estimating a diameter ratio (the ratio of the diameter of the smaller spheroid to the diameter of the larger spheroid). The very large budded, uninucleate class (see Fig. 2) was defined as those cells with a diameter ratio of >0.75 and with a single DAPI staining region located entirely within the neck proximal hemisphere. Precision and accuracy of the visual estimations were determined by photography using two methods. In the first, a random sample of fixed cells from YPH631 (a yeast strain containing a CF with CDEII $\Delta 31$ *CEN6*) was photographed, the scored class was identified by visual inspection, and then spheroid diameters were measured. Eighteen cells out of 206 (8.7%) were scored positive by visual estimate, with an average diameter ratio of 0.8 (range of 0.8–1.0). In the second, individual cells of the scored class were photographed at higher magnification for more precise measurement of sphere diameters. In a sample of 38, the mean sphere diameter ratio \pm SD was 0.85 ± 0.08 (range 0.69–1.0), including only three false positives (one with a ratio of 0.69 and two with a ratio of 0.71).

Several control strains containing CFs with wild-type *CEN6* alleles but differing in auxotrophic markers were characterized (YPH816, YPH281, and YPH817). No significant difference in the frequency of very large budded, uninucleate cells was observed.

Viable Cell Characterization at Cell Separation. Yeast in logarithmic growth in liquid minimal medium without uracil (selecting for the CF) were transferred to solid rich medium (with no selection), and cells with small buds were micro-manipulated to defined positions by using a glass needle (as in ref. 21). Each cell was checked for mother–bud separation every 30 min (room temperature) by micromanipulation. At

cell separation, the relative sizes of the two cells were characterized as a spheroid diameter ratio. The products of the scored cell division were left in defined positions and allowed to form colonies. Two rare classes of cell divisions were omitted from the data: (i) the case in which one or both daughter cells failed to form a colony, and (ii) the case in which the observed division probably took place in the absence of a CF (neither mother nor daughter inherited a CF).

Characterization of Cell Cycle Progression in Synchronous Populations. Exponential phase yeast ($\approx 2.5 \times 10^6$ cells per ml) cultured in minimal medium lacking uracil were pelleted in a brief centrifugation and resuspended in yeast extract/peptone/dextrose at a similar density. After a 2-hr culture, haploid *MATa* cells were arrested in G_1 by addition of α mating pheromone (final concentration of 3 μ M; Sigma). Two hours postaddition, cells were released by return to fresh yeast extract/peptone/dextrose. Aliquots taken every 5 or 10 min were fixed by addition of 1/10th volume of 37% formaldehyde (Sigma) directly to the culture medium and overnight incubation at room temperature. Cell samples were prepared for flow cytometry (22). DNA content profiles of propidium iodide-stained samples were obtained using a Coulter EPICS flow cytometer, and cellular nuclear morphology was determined by using simultaneous epifluorescence and phase microscopy.

RESULTS

We have characterized a series of yeast strains that contain *CEN* DNA mutations partially disrupting chromosome transmission fidelity for the presence of cell cycle alterations. The test chromosome in this panel of strains is a CF, an independently segregating linkage group that is not essential for viability on nonselective medium (16). The CF diagrammed in Fig. 1 is maintained (15) with mitotic stability (1 loss per 2×10^4 divisions) that approaches that of yeast natural chromosome III (1 loss per 10^5 divisions; refs. 23 and 24). Replacement of the wild-type *CEN* DNA with mutant *CEN* DNAs results in an otherwise isogenic series of strains well suited for describing the effects of *CEN* DNA structural alterations (and hence kinetochore defects) on progression through the cell cycle.

Cell Cycle Alteration in Logarithmic Populations. A morphological screen for altered cell cycle progression was employed in the characterization of yeast strains carrying one mutant centromere on a CF. Yeast in logarithmic growth were fixed in formaldehyde and stained with the DNA-binding dye DAPI. Samples were scored for the frequency of morphological classes based on bud size, nuclear number, and nuclear location. An alteration in the cell cycle of some mutant strains was observed as an accumulation of cells with very large buds and an undivided nucleus at the neck (Fig. 2). This cellular morphology is typical of temperature-sensitive

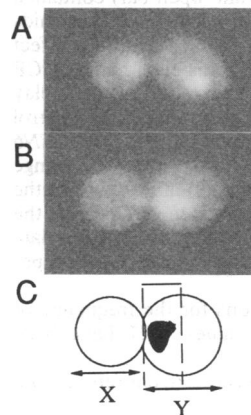


FIG. 2. (A) The predominant post-anaphase morphology seen in control strains. (B) The mitotic delay morphology, in which the bud diameter is unusually large though anaphase separation has not occurred (magnification identical to that in A). (C) The scoring criteria included a requirement for (i) nucleus at the neck (when the DAPI staining region was entirely within the neck proximal 50%), and (ii) very large bud morphology (when $X > 0.75 Y$).

mutants that exhibit a homogeneous arrest in G₂ or early M (some of the *cdc* mutants; ref. 25), reflecting cytoplasmic growth that has advanced beyond the stage normally achieved at the time of nuclear division. The observation of similar abnormally large budded, uninucleate cells in logarithmically growing populations suggests that nuclear events in some (or all) cells are occurring behind schedule, and the cell cycle alteration is revealed as delayed mitosis. We will hereafter refer to this as a “mitotic delay” morphology, an interpretation supported by flow cytometry of synchronous cell populations (see below).

Quantitative experimental results for the panel of strains are summarized in Fig. 3. The uninucleate, very large budded morphology is observed in ≈1% of cells in a control strain in which the CF carries a wild-type *CEN*. The strongest cell cycle alteration is seen in the yeast strain harboring CDEII Δ31 (a 31-base-pair deletion within CDEII; ref. 38). This strain exhibits an 8-fold increase in the number of mitotically delayed cells within a logarithmic culture: 1 in 12 cells exhibits the mitotic delay morphology in the presence of this *CEN* DNA mutation, in contrast to 1 in 100 cells of the control

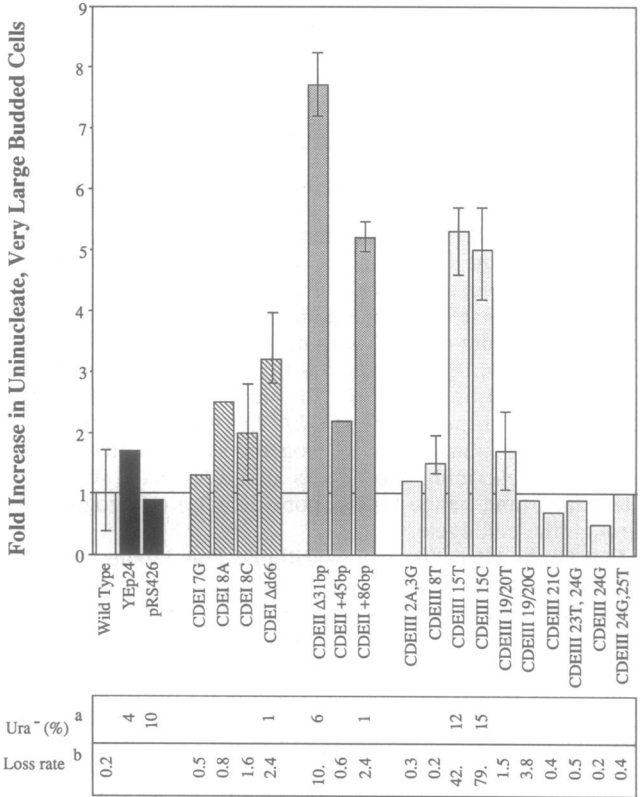


FIG. 3. The mitotic delay observed in the presence of various *CEN6* mutations is shown. The control strain (open bar) contained a CF carrying a wild-type *CEN6*. Strains with the 2-μm plasmids YEp24 and pRS426 (solid bars) were included to measure the effect of auxotrophic starvation. The remaining strains each harbor a CF with the indicated *CEN6* mutation. Fold increase = % mitotic delay class in the experimental strain/% mitotic delay class in the control strain. The observed frequency in the presence of wild-type *CEN6* was 1.2% ± 0.5% (± SD with 12 df); error bars show the range observed in 13 measurements. For data from strains containing the *CEN* mutations, the error bars (on the arithmetic mean) indicate the range observed for determinations made in triplicate; other data points represent single measurements. The minimum sample size per measurement was 800 cells.

^a Data are the average of two determinations for the frequency of uracil auxotrophs in selective culture; values <1% have been omitted.
^b Loss rate is shown as events per 1000 divisions (from refs. 15 and 16).

culture. Additional centromere mutations with clearly significant effects include CDEII +86bp (tandem duplication of CDEII), CDEIII 15T and CDEIII 15C (nucleotide substitutions at position 15 of CDEIII), and CDEI Δ (CDEI deletion). Other centromere mutations tested do not exhibit clearly detectable delays by this assay.

To maximize the number of cells in culture containing the mutant centromere, all yeast strains in the above experiments were grown in medium selecting for the CF marker conferring uracil prototrophy. It was possible that the accumulated class represented the uracil-starved auxotrophs that had lost the CF. The contribution of starving cells was addressed by characterization of yeast strains containing *URA3*-marked 2-μm plasmids [YEp24 (26) or pRS426 (27)]. The frequency of uracil-starved cells in these 2-μm containing strains was similar to that observed in strains containing the most unstable CF tested (Fig. 3), yet the frequency of very large budded, uninucleate cells is equivalent to that seen in the presence of the CF with wild-type *CEN6*.

Delay Associated with the Mutant *CEN*. The mitotic delay phenotype has been characterized in a series of otherwise isogenic yeast strains that carry a single extra chromosome whose *CEN* DNA has been mutated. Thus, the cell cycle delay is formally due to the alteration in the *CEN* DNA and presumably due to the defective assembly or function of the kinetochore proteins assembled on the mutant site. However, a potential caveat to this interpretation stems from the possible accumulation of CFs with mutant *CEN* DNAs by nondisjunction. If this occurs, the cell cycle alteration could be due to an increase in copy number of any sequence on the CF.

Direct experimental evidence that the delay is due to the presence of the mutant *CEN* itself was obtained by characterizing the effect of *CEN6* CDEII Δ31 on a YAC. The structure of this YAC (Fig. 1) is such that the yeast chromosome III long arm of the CF is replaced with anonymous human DNA, and the *SUP11* gene has been deleted from the short arm. The YAC retains use of the *URA3* prototrophic marker for selection, already well characterized in the 2-μm experiment. Very large budded, uninucleate cells were observed at a frequency 6.6-fold higher in the presence of *CEN6* CDEII Δ31 (9.9% in YPH815) than in the presence of a wild-type *CEN6* (1.5% in YPH814). Generalizing from these results, we conclude that the mitotic delay is due to the presence of the *CEN* DNA mutation itself.

Cell Cycle Alteration in Individual Cell Cycles. The data from fixed logarithmic phase populations demonstrate the existence of a cell cycle delay but do not distinguish between a small alteration exhibited by all cells, a longer delay exhibited by a rare subpopulation of cells, or an intermediate condition. To address this issue, budded cells were micro-manipulated to defined positions on rich solid media, and relative cell size at separation was noted for a large number of individual cell divisions. This provided direct quantitation of the proportion of cells that delay sufficiently to produce very large budded cells (bud diameter ≥three-fourths that of the mother) before separation.

In general, at cell separation in the control, the daughter cell was released as a smaller spheroid, with a diameter usually less than three-fourths that of the mother (Table 1). Yeast strains containing *CEN* mutants exhibiting a delay in the fixed cell morphological screen also show a delay in this assay (CDEII Δ31, CDEIII 15T, and CDEII +86bp) and appear to delay in the same affected order. One *CEN* mutant (CDEII +45bp) with no (or slight) effect in the fixed cell morphological screen exhibited the very large bud class at a frequency indistinguishable from the control. For one mutant (CDEII Δ31), a segregant lacking the CF served as a control, demonstrating the dependence of very large bud formation on the presence of the CF.

Table 1. Relative bud size in individual mitoses

Strain	CF <i>CEN</i> allele	<i>n</i>	Diameter ratio ≤ 0.75	Diameter ratio > 0.75
YF144	Wild type	131	0.92	0.08
YF144R*	No CF	94	0.95	0.05
YPH631	CDEII $\Delta 31$ bp	124	0.41	0.59
YPH631R*	No CF	86	0.95	0.05
YPH630	CDEII +45bp	89	0.91	0.09
YPH773	CDEII +86bp	45	0.80	0.20
YPH291	CDEIII 15T	71	0.73	0.27

n, number of divisions monitored. The values given in columns 4 and 5 are the fraction of daughter cells with a diameter ratio ≤ 0.75 or > 0.75 , respectively.

*YF144R and YPH631R are mitotic segregants lacking the CF, derived from single colonies of strains YF144 and YPH631, respectively.

In yeast containing CDEII $\Delta 31$, the bud achieves an increased diameter detected by the assay limit in over half of all divisions. This observation leads to two important conclusions. First, cells that achieve very large bud size in culture are undergoing productive cell cycles and do not represent terminal events. Second, in the presence of CDEII $\Delta 31$, most (and possibly all) cells experience delay in each cycle. This latter conclusion supports the argument that the delay cannot be attributed to an increase in CF number (only 5–10% of the cells containing CDEII $\Delta 31$ have ≥ 2 CFs).

Cell Cycle Alteration in Synchronous Populations. The advanced bud growth observed in fixed cell populations, and in viable cells at separation, strongly suggests that the progress of nuclear events lags behind that of cytoplasmic events. However, these observations alone do not address the issue of when in the cell cycle the nucleus falls behind the cytoplasm. Because most cells containing CDEII $\Delta 31$ undergo delay, we chose to monitor the nuclear cycle in a cell population synchronized by release after mating pheromone-induced arrest in G₁.

Aliquots taken after release from α factor arrest in the G₁ phase of the cell cycle were subjected to flow cytometry (Fig. 4) and morphological analysis (Fig. 5). The flow cytometric histogram profiles (Fig. 4A) for the experimental (YPH429, with *CEN6* CDEII $\Delta 31$) and control (YPH427, with wild-type *CEN6*) strains were virtually identical at arrest and at early

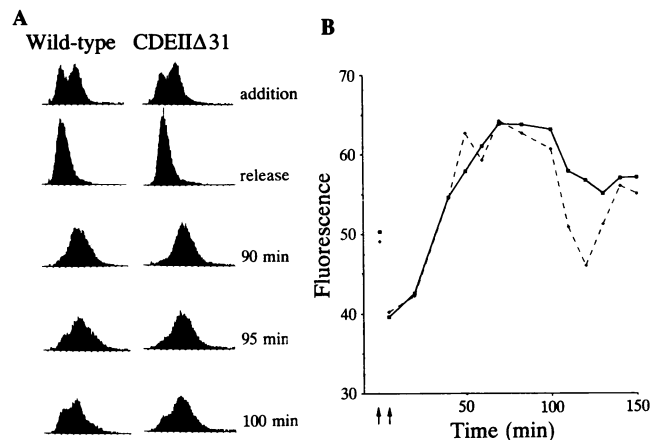


FIG. 4. (A) Flow cytometry histograms (number of cells vs. propidium iodide fluorescence) showing the distribution of cells at α factor addition, at release from the α factor block, and at the times when the profiles in the presence of wild-type and mutant *CEN* become visibly different. (B) The mean fluorescence of each time point reflects the mean cell cycle position of the cell population. Dashed line, cells containing the CF with wild-type *CEN6*; solid line, cells containing CDEII $\Delta 31$ *CEN6*. Arrows indicate α factor addition and removal.

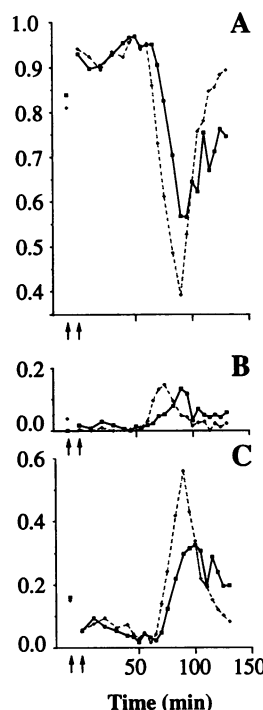


FIG. 5. The frequencies of cells with one spherical chromosomal mass (A), one elongate chromosomal mass (B), or two separated chromosomal masses (C) are shown. The minimum sample size per measurement was 400 cells. Dashed line, cells containing the CF with wild-type *CEN6*; solid line, cells containing the CDEII $\Delta 31$ *CEN6*. Arrows indicate α factor addition and removal.

times after release through the period in which DNA synthesis occurred. The profiles became visibly different at about 95 min postrelease, at which time the production of G₁ cells by cell division clearly occurred later in the presence of CDEII $\Delta 31$. A simple plot of the average DNA content per cell (Fig. 4B) graphically demonstrates this delay and indicates a decrease in synchrony by the second cell cycle within the *CEN* mutant-containing strain. We conclude that, in the presence of CDEII $\Delta 31$, progress is phenotypically normal with respect to bulk DNA synthesis through S phase and that a delay is revealed between late S phase and cell separation.

Morphological characterization of these same synchronous samples was performed (Fig. 5). Each cell was scored in one of three categories: cells with one roughly spherical nucleus (regardless of bud morphology), cells with an elongate nucleus (i.e., cells in mitosis), and cells with two nuclei (after chromosome separation). Cell cycle progress by these measures also exhibits a delay. The decay in the frequency of cells with one nucleus occurs later in the presence of the CDEII $\Delta 31$ mutation, as does the appearance of cells with one elongate nucleus or two nuclei. Taken together with the flow cytometry profiles, these data delimit the appearance of the delay to a time between late S phase and chromosome separation in mitosis. Furthermore, an average duration of the delay can be estimated from the difference in the times at which cells in mitosis appear as the separation between the peak frequencies of cells with elongated nuclei (Fig. 4B). This difference is ≈ 10 min, which indicates a delay representing about 10% of the normal cell cycle.

DISCUSSION

These data identify a cellular response to the presence of a *CEN* DNA lesion carried by a single chromosome in yeast. Previous studies have raised the possibility that centromere sequences may have deleterious effects on growth when present at high copy number (refs. 28 and 29, but see ref. 30), on dicentric chromosomes (31–33), or on linear minichromosomes (39). In contrast, this study identifies a delay-inducing potential of mutant centromere DNA sequences in an experimental system in which each tested mutant centromere is present at single copy on a chromosome demonstrated to

contain all other structural requirements for stable transmission. It is important to note that the primary cause of the delay (the "execution point" of the defect; ref. 25) may occur prior to its appearance, but must occur before nuclear separation. The dependence on the presence of *CEN* DNA lesions, and occurrence between late S phase and chromosome separation, strongly favors a model in which the primary cause of the delay is misassembly of kinetochore proteins and ensuing defective spindle attachment.

It is possible that the mitotic delay serves to stabilize chromosomes with mutant centromeres. The presence of a stabilizing function for chromosomes with abnormal kinetochores would have consequences for interpretation of mitotic instability phenotypes engendered by *CEN* DNA mutants; some potential loss events may be remedied by a delay prior to the onset of anaphase. The observations reported here do not define a functional relationship between the delay and chromosome stability, but do indirectly address the issue. We note that the marker chromosome containing the *CEN6* CDEII $\Delta 31$ mutation will undergo mitotic loss in only 1 of 100 cell divisions (15), whereas a majority (>50%) of cell cycles exhibit delay in the presence of this *CEN* mutant. This observation is inconsistent with models in which delay occurs only in those cell cycles that will fail in proper segregation of the mutant centromere. We also observe that the magnitude of centromere defect as measured by mitotic instability does not relate in linear fashion with the magnitude of delay. For example, CDEII $\Delta 31$ causes a 50-fold increase in missegregation and shows an 8-fold increase in very large budded, uninucleate cells, whereas CDEIII 15T causes a 500-fold increase in missegregation and shows a 5-fold increase in very large budded, uninucleate cells. Thus, the delay-inducing potential of a kinetochore abnormality is not a simple function of its chromosome segregation defect.

It is remarkable that a single mutant *CEN*, in the presence of 32 normal centromeres on the natural chromosomes, can lead to a mitotic delay. In theory, the delay might be due to a structural defect that slows the progress of a rate-limiting step in the required series of nuclear events or to the action of an extrinsic surveillance system that monitors the completion of some processes at a checkpoint before allowing the initiation of subsequent events (1). Characterization of the gene products required for this delay will address this question. Several genetic loci have recently been identified (6, 7) in yeast for their inability to cause arrest or delay in the presence of microtubule-destabilizing drugs and provide excellent candidates for mutants involved in spindle surveillance.

The similarity between the delay observed in response to an unattached chromosome during prometaphase spindle attachment in animal cells and this phenomenon in yeast is provocative. While the cytological description of the behavior of chromosomes throughout the cell cycle is vastly superior in animal systems, the observation of similar phenomena in yeast opens avenues to efficient molecular genetic approaches. The structure and function of the yeast kinetochore (*CEN* DNA sequence and associated proteins) is currently the subject of intensive investigation in many laboratories (34–37, 40, 41). Moreover, the identification of mutant yeast defective in the cellular response to *CEN* DNA lesions should lead to the characterization of proteins involved in controlling the progress of events occurring at the kinetochore. If these controlling functions are well conserved in evolution, study of the yeast gene products may in the future provide reagents for the molecular analysis of cytological phenomena observed in animal cells. It is possible that loss of temporal controls governing events at the kinetochore may contribute to karyotypic instability, resulting in aneuploidy-associated cellular defects and organismal disease states.

The authors are especially grateful for stimulating discussions with J. Hegemann. We thank S. Desiderio, W. Earnshaw, G. Kettner, D. Koshland, and R. Reed for critical reading of the manuscript; D. Sears for unpublished strains; and J. Flook for assistance with the flow cytometry. This work was supported by grants from the American Cancer Society (IRG-11-30 to F.S.) and the National Institutes of Health (CA16519 to P.H.).

- Hartwell, L. & Weinert, T. (1989) *Science* **246**, 629–634.
- Weinert, T. & Hartwell, L. (1988) *Science* **241**, 317–322.
- Weinert, T. & Hartwell, L. (1990) *Mol. Cell. Biol.* **10**, 6554–6564.
- Elion, E., Gisafi, P. & Fink, G. (1990) *Cell* **60**, 649–664.
- Chang, F. & Herskowitz, I. (1990) *Cell* **63**, 999–1011.
- Hoyt, M. A., Totis, L. & Roberts, T. (1991) *Cell* **66**, 507–517.
- Li, R. & Murray, A. (1991) *Cell* **66**, 519–531.
- Nurse, P. (1990) *Nature (London)* **344**, 503–508.
- Rieder, C. & Alexander, S. (1989) in *Mechanisms of Chromosome Distribution and Aneuploidy*, eds. Resnick, M. & Vig, B. (Liss, New York), pp. 185–194.
- Zirkle, R. (1970) *Radiat. Res.* **41**, 516–537.
- Nicklas, R. (1967) *Chromosoma* **21**, 17–50.
- Rieder, C. (1982) *Int. Rev. Cytol.* **79**, 1–58.
- Byers, B. (1981) in *The Molecular Biology of the Yeast Saccharomyces: Life Cycle and Inheritance*, eds. Strathern, J., Jones, E. & Broach, J. (Cold Spring Harbor Lab., Cold Spring Harbor, NY), pp. 59–96.
- Newlon, C. (1988) *Microbiol. Rev.* **52**, 568–601.
- Hegemann, J., Shero, J., Cottarel, G., Philippsen, P. & Hieter, P. (1988) *Mol. Cell. Biol.* **8**, 2523–2535.
- Shero, J., Koval, M., Spencer, F., Palmer, R., Hieter, P. & Koshland, D. (1991) *Methods Enzymol.* **194**, 749–773.
- Shero, J. & Hieter, P. (1991) *Genes Dev.* **5**, 549–560.
- Shero, J. (1989) Ph.D. thesis (The Johns Hopkins Univ., Baltimore).
- Sears, D., Hegemann, J. & Hieter, P. (1992) *Proc. Natl. Acad. Sci. USA* **89**, 5296–5300.
- Rose, M., Winston, F. & Hieter, P. (1990) *Methods in Yeast Genetics* (Cold Spring Harbor Lab., Cold Spring Harbor, NY).
- Murray, A. & Szostak, J. (1983) *Cell* **34**, 961–970.
- Hutter, K. J. & Eipel, H. E. (1978) *Antonie von Leeuwenhoek Microbiol. Serol.* **44**, 269–282.
- Hartwell, L., Dutcher, S., Wood, J. & Garvik, B. (1982) *Recent Adv. Yeast Mol. Biol.* **1**, 28–38.
- Hartwell, L. & Smith, D. (1985) *Genetics* **110**, 381–395.
- Pringle, J. & Hartwell, L. (1981) in *The Molecular Biology of the Yeast Saccharomyces: Life Cycle and Inheritance*, eds. Strathern, J., Jones, E. & Broach, J. (Cold Spring Harbor Lab., Cold Spring Harbor, NY), pp. 97–142.
- Botstein, D., Falco, S. C., Stewart, S., Brennan, M., Scherer, S., Stinchcomb, D., Struhl, K. & Davis, R. (1979) *Gene* **8**, 17–24.
- Christianson, T., Sikorski, R., Dante, M., Shero, J. & Hieter, P. (1992) *Gene* **110**, 119–122.
- Futcher, B. & Carbon, J. (1986) *Mol. Cell. Biol.* **6**, 2213–2222.
- Runge, K., Wellinger, R. & Zakian, V. (1991) *Mol. Cell. Biol.* **11**, 2919–2928.
- Smith, D., Smyth, A. & Moir, D. (1990) *Proc. Natl. Acad. Sci. USA* **87**, 8242–8246.
- Koshland, D., Rutledge, L., Fitzgerald-Hayes, M. & Hartwell, L. (1987) *Cell* **48**, 801–812.
- Hill, A. & Bloom, K. (1989) *Mol. Cell. Biol.* **9**, 1368–1370.
- Neff, M. & Burke, D. (1992) *Mol. Cell. Biol.*, in press.
- Baker, R. & Masison, D. (1990) *Mol. Cell. Biol.* **10**, 2458–2467.
- Cai, M. & Davis, R. (1990) *Cell* **61**, 437–446.
- Mellor, J., Jiang, W., Funk, M., Rathjen, J., Barnes, C., Hinz, T., Hegemann, J. & Philippsen, P. (1990) *EMBO J.* **9**, 4017–4026.
- Lechner, H. & Carbon, J. (1991) *Cell* **64**, 717–725.
- Panzeri, L., Landonio, L., Stotz, A. & Philippsen, P. (1985) *EMBO J.* **4**, 1867–1874.
- Murray, A. W. (1991) *Cold Spring Harbor Symp. Quant. Biol.* **56**, 399–408.
- Niedenthal, R., Stoll, R. & Hegemann, J. (1991) *Mol. Cell. Biol.* **11**, 3545–3553.
- Jehn, B., Niedenthal, R. & Hegemann, J. (1991) *Mol. Cell. Biol.* **11**, 5212–5221.